

# Anatomic Study of the Canine Stifle Using Low-Field Magnetic Resonance Imaging (MRI) and MRI Arthrography

Esteban Pujol<sup>1</sup>, DVM, Henri Van Bree<sup>2</sup>, DVM, PhD, Diplomate ECVI, Diplomate ECVS, Laurent Cauzinille<sup>1</sup>, DVM, Diplomate ACVIM (Neurology), Cyrill Poncet<sup>1</sup>, DVM, Diplomate ECVS, Ingrid Gielen<sup>2</sup>, DVM, PhD, and Bernard Bouvy<sup>1</sup>, DVM, MS, Diplomate ACVS/ECVS

<sup>1</sup>Small Animal Surgery Department, Centre Hospitalier Vétérinaire Frégis, Arcueil, France and <sup>2</sup>Department of Medical Imaging of Domestic Animals, Faculty of Veterinary Medicine, Ghent University, Merelbeke, Belgium

## Corresponding Author

Esteban Pujol DVM, Small Animal Surgery Department, Centre Hospitalier Vétérinaire Frégis, 43 avenue Aristide Briand, 94110, Arcueil, France  
E-mail: estebanpujol@gmail.com

Submitted February 2010

Accepted May 2010

DOI:10.1111/j.1532-950X.2011.00823.x

**Objective:** To investigate the use of low-field magnetic resonance imaging (MRI) and MR arthrography in normal canine stifles and to compare MRI images to gross dissection.

**Study Design:** Descriptive study.

**Sample Population:** Adult canine pelvic limbs (n = 17).

**Methods:** Stifle joints from 12 dogs were examined by orthopedic and radiographic examination, synovial fluid analysis, and MRI performed using a 0.2 T system. Limbs 1 to 7 were used to develop the MR and MR arthrography imaging protocol. Limbs 8–17 were studied with the developed MR and MR arthrography protocol and by gross dissection. Three sequences were obtained: T1-weighted spin echo (SE) in sagittal, dorsal, and transverse plane; T2-weighted SE in sagittal plane and T1-gradient echo in sagittal plane.

**Results:** Specific bony and soft tissue structures were easily identifiable with the exception of articular cartilage. The cranial and caudal cruciate ligaments were identified. Medial and lateral menisci were seen as wedge-shaped hypointense areas. MR arthrography permitted further delineation of specific structures. MR images corresponded with gross dissection morphology.

**Conclusions:** With the exception of poor delineation of articular cartilage, a low-field MRI and MR arthrography protocol provides images of adequate quality to assess the normal canine stifle joint.

Magnetic resonance imaging (MRI) is currently one of the most effective diagnostic tools for assessment of joint disorders and has led to a better understanding of normal anatomy and pathologic features in people.<sup>1</sup> The soft tissue image resolution, the ability to image in multiple planes and the absence of ionizing radiation have made MRI the diagnostic modality of choice for traumatic, degenerative, and inflammatory diseases of joints in people.<sup>2,3</sup> It is the only noninvasive modality that allows combined evaluation of articular cartilage, subchondral bone, and soft tissue structures associated to the joint. Moreover, in human medicine MRI of the knee is reported to be the most common non-neurologic application<sup>4</sup> and detection of meniscal tears,<sup>5</sup> ligament tears,<sup>6</sup> and cartilage lesions<sup>7</sup> has been reported.

MR arthrography is more invasive than conventional MRI, but provides additional information about the integrity of joint structures, especially cartilaginous and ligamentous abnormalities. In people, indications for MR

arthrography include evaluation of articular cartilage, menisci, identification of intraarticular loose bodies, evaluation of osteochondritis dissecans and diagnosis of recurrent meniscal tears after meniscal surgery.<sup>8–11</sup> MR arthrography can be considered supplemental to conventional MR study or, may be the preferred initial examination.<sup>1,8,10</sup>

High- and low-field MRI has been used for detection of intraarticular lesions and for diagnostic investigation of stifle injuries and degenerative changes in small animals. High-field MRI is more sensitive than computed radiography in assessing onset and progression of degenerative changes in canine experimental osteoarthritis and provided discrimination between joint effusion and synovial thickening.<sup>12</sup> High-field MRI provided a sensitivity of 100% for the diagnosis of a meniscal tear in naturally occurring cranial cruciate injury in dogs.<sup>13</sup> High-field MR arthrography study in military dogs identified pathologic meniscal changes.<sup>14</sup> Low-field MRI allowed detection of early subchondral bone changes (as early as 2 weeks) in induced cranial cruciate ligament deficiency in dogs.<sup>15</sup> Low-field MRI of meniscal lesions correlated well with arthroscopy and necropsy findings in another canine study.<sup>16</sup> There are few reports on high- or low-field

Presented in part at the 18th Annual Scientific Meeting ECVS 2009, Nantes, France.

MRI of the normal canine stifle<sup>17,18</sup>; carpus<sup>19</sup>; elbow<sup>20</sup>; and shoulder.<sup>21</sup> The lower signal to noise ratio of low-field systems requires a relatively long acquisition time and requires thicker slices to produce images of acceptable quality. Spatial resolution is also reduced with low field compared with high-field systems, whether this difference in spatial resolution is clinically important in dogs is unknown until studies comparing high- and low-field systems are reported. Nevertheless, low-field MRI machines recently made available for practitioners have advantages including presence of the anesthetic equipment in the same room, open design for easy patient positioning, and lower equipment purchase and maintenance expenses.<sup>17</sup>

There are few reports of the use of CT or CT arthrography in the canine stifle.<sup>22,23,24</sup> The results for identifying simulated meniscal injury are encouraging<sup>22</sup>; however, 2 clinical studies questioned the value of CT arthrography for detection of naturally occurring meniscal injuries.<sup>23,24</sup> As in people, MR contrast arthrography may improve noninvasive observation of intraarticular stifle structures (menisci, ligaments), tendons, and articular margins in dogs. We are only aware of 1 report of MR arthrography of the canine stifle joint using a high-field MRI unit.<sup>10</sup> Stifle study using low-field MRI combined with MR arthrography in normal dogs has not been reported.

Our purpose was (1) to develop a protocol for stifle MRI and MR arthrography in normal dogs using a low-field magnet; (2) to describe low-field MRI anatomy of the normal stifle and to compare findings with gross dissection observations in cadaveric limbs; and (3) compare conventional MR and MR arthrography images of the normal stifle.

## MATERIALS AND METHODS

Pelvic limbs ( $n = 17$ ) from 12 dogs euthanatized for reasons unrelated to stifle disease were studied. Stifles were considered normal based on physical orthopedic examination, radiographic examination (mediolateral and caudocranial projections), and joint fluid analysis ( $< 2$  mononucleated cells/ $\mu\text{L}$ ) performed while the dogs were anesthetized, and later by gross dissection.

Dogs were administered diazepam (0.2 mg/kg intravenously [IV]), anesthetized with propofol (4 mg/kg IV) and maintained with isoflurane in oxygen. MRI was performed with a 0.2T system (Esaote Vet MR, Genova, Italy). Different dog positions were experienced before standardizing the protocol. Dogs were positioned in lateral recumbency with the upper stifle in  $145^\circ$  of flexion. A rigid coil intended for examining the human elbow was used (Fig 1). Three image sequences were used: a T1-weighted spin echo (SE) sequence (660 TR 26 TE; NEX 4; matrix  $192 \times 115$ ; FOV  $200 \times 180$  mm; pixel dimension  $1.57 \text{ mm} \times 1.04 \text{ mm}$ ; time 4 minutes) in sagittal, dorsal, and transverse planes; a T2-weighted SE sequence (920 TR 26 TE; NEX 4; matrix  $288 \times 173$ ; FOV  $200 \times 180$  mm; pixel dimension  $1.04 \text{ mm} \times 0.7 \text{ mm}$ ; time 10 minutes) in sagittal plane and a T1-gradient echo (GE) sequence (600 TR 16 TE; NEX 4;



**Figure 1** Rigid extremity coil used for this study.

matrix  $288 \times 173$ ; FOV  $200 \times 180$  mm; pixel dimension  $1.04 \text{ mm} \times 0.7 \text{ mm}$ ; time 8 minutes) in sagittal plane. This resulted in images with a 4 mm slice thickness with 0.4 mm of interslice gap. Different orientations of the sagittal, transverse, and dorsal planes were tried before standardizing the protocol. Using a 30-second acquisition T1-weighted SE sequence, the sagittal plane was set to be parallel with the plane of the cranial cruciate ligament; the dorsal plane was set parallel to the patellar ligament, and the transverse sequences were set parallel to the tibial plateau.

After the precontrast sequences, a solution of diluted gadopentate (Magnevist, gadopentate dimeglumine, 469.01 mg/mL; 1 mL gadopentate was diluted in 100 mL 0.9% sodium chloride solution<sup>14</sup>) was introduced by lateral parapatellar injection (20 G needle, 20 mL syringe) into the stifle until palpable distension of the articular capsule (10–15 mL). The stifle was then flexed and extended several times to distribute fluid within the joint. Postcontrast images were acquired using the same sequences except for the T2-weighted SE. Total imaging time for both studies (MR+MR – arthrography) was  $< 75$  min/stifle.

Limbs 1 to 7 were used to develop the MR and MR arthrography imaging protocol. Limbs 8–17 were studied using the developed MR and MR arthrography protocol and by gross dissection. Systematic anatomic review was conducted for each MR examination and included periarticular muscles, joint capsule, patella and patellar tendon, cranial and caudal cruciate ligaments, femoral condyles, articular cartilage, subchondral bone, medial and lateral menisci, extensor fossa, sesamoid bones, and meniscal ligaments. The images of pre- and postcontrast studies were matched and compared.

Dogs were euthanatized with sodium pentobarbital after MRI without recovery from anesthesia. Limb dissection was performed immediately after euthanasia in a reproducible manner. All extra/intraarticular structures described earlier were checked. Collateral ligaments, cruciate

ligaments, and meniscofemoral ligament were transected with care to “open” the stifle in an atraumatic manner. All menisci were removed to look for abnormalities on their distal surface.

Data obtained from anatomic structures was recorded and digital photographs were taken. Findings from gross dissection were compared with MR and MR arthrography images to ascertain the lack of abnormalities. Menisci from 6 stifles were examined by histopathology (4% formalin fixation; 2 µm sections stained with hematoxylin–eosin).

**RESULTS**

Ten hind limbs from 8 medium and large breed dogs were included. Mean weight was 40.5 kg (median, 35 kg; range, 20–47 kg). Mean age was 11.1 years (median, 12 years; range, 7–13 years). Breeds were Doberman (2), Labrador retriever (2), and 1 each of German short-hair pointer, Rhodesian Ridgeback, German Shepherd, and Beauceron. Seven left and 3 right stifles were evaluated.

*MR Findings*

On all limb images, specific bony and soft tissue structures were easily identifiable (signal intensities by MRI sequences, Table 1), except articular cartilage. Extraarticular structures (muscles, bones, tendons, and ligaments) were clearly visible for each stifle in all sequences. Semitendinosus, semimembranosus, and gastrocnemius muscles were observed as intermediate signal intensity structures, better defined with sagittal T1-weighted GE sequence (Fig 2A). A thin hypointense band at the peripheral margins of the muscles and cartilage (or joint capsule) was seen on T1-weighted GE sequences. The patella had intermediate signal intensity in all sequences because of bone marrow. In the 3 planes and in all sequences, the patella was delineated by a low-intensity signal corresponding to cortical bone. The femoral condyles and sesamoid bones were easily evaluated in dorsal and sagittal planes, with intermediate intensity signal. The patellar tendon had low signal intensity

in all sequences. The infrapatellar fat pad appeared hyperintense in all sequences (Fig 2B). The tendon of the long digital extensor muscle could be seen on transverse and sagittal planes with low signal intensity. The collateral ligaments were observed as low signal bands in dorsal and transverse planes.

The cranial and caudal cruciate ligaments were systematically identified as 2 low homogeneous intensity oblique bands in all sequences, better seen in sagittal and dorsal planes. The cranial cruciate ligament could not be seen in its entirety in the same image in all stifles. The caudal cruciate was more frequently seen in its entirety in a single image (Fig 2C and D).

Medial and lateral menisci of all limbs were seen as wedge-shaped areas of low signal intensity in dorsal and sagittal plane (Fig 2E and F). An inhomogeneous increase of central intrameniscal signal without extension to the periphery was seen in GE sequence in 8 joints (Fig 2G). The caudal horn of lateral meniscus was difficult to see in some dogs, because of interference with popliteus tendon insertion zone.

The articular cartilage itself was not clearly identified in any stifle. A combination of joint fluid and articular cartilage was identified as high signal intensity line in T2-SE (Fig 2E item “k”) and even better in GE sequences (Fig 2G item “k”). In both sequences, the combination of articular cartilage and joint fluid was separated from trabecular bone by a hypointense line that corresponded to subchondral bone.

*MR Arthrography*

MR arthrography improved identification of some structures. The meniscofemoral ligament was identified as a linear oblique band of low signal intensity between the caudal part of the lateral meniscus and the medial femoral condyle dorsally in the dorsal plane (Fig 3A, A', and A''). The joint capsule was better observed than with noncontrast MRI in all stifles (Fig 3B). The cranial and caudal cruciate ligaments were better defined than in conventional MRI in most dogs and were seen as low signal intensity bands. The

**Table 1** Summary of the MR intensities of Different Structures in Each Sequence

	T1	T2	GE
Muscles	Intermediate	Intermediate	Intermediate
Patella	Intermediate	Intermediate	Intermediate
Patellar tendon	Hypointense	Hypointense	Hypointense
Infrapatellar fat pad	Hyperintense	Hyperintense	Hyperintense
Long digital extensor tendon	Hypointense	Hypointense	Hypointense
Collateral ligament	Hypointense	Hypointense	Hypointense
Femoral condyles	Intermediate	Intermediate	Intermediate
Sesamoid bones	Intermediate	Intermediate	Intermediate
Cruciate ligaments	Hypointense	Hypointense	Hypointense
Meniscal horn	Hypointense	Hypointense	Hypointense
Central part of the menisci	Hypointense	Hypointense	Hyperintense (8/10)
Joint fluid-articular cartilage	Hypointense	Hyperintense	Hyperintense
Subchondral plate	Hypointense	Hypointense	Hypointense
Bone marrow	Intermediate	Intermediate	Intermediate

GE, gradient echo; MR, magnetic resonance.

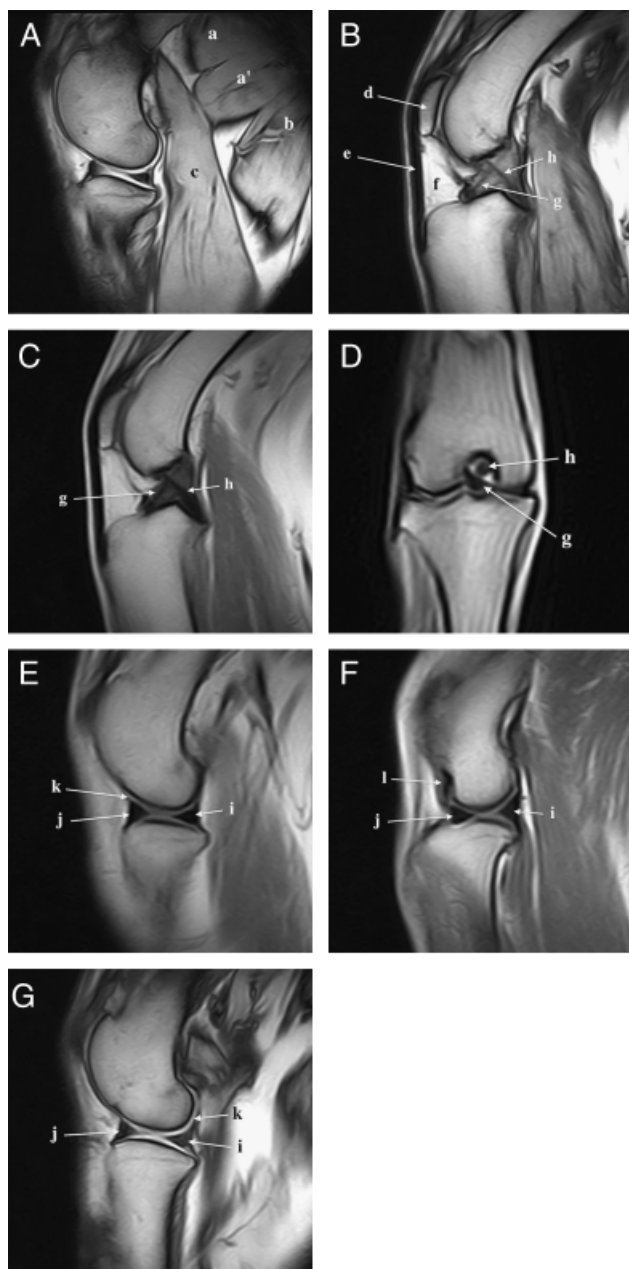


**Figure 2** (A) Sagittal T1 gradient echo (GE) image of the medial joint compartment: a, semimembranosus muscle, cranial (a) and caudal (a') belly; b, semitendinosus muscle; c, gastrocnemius muscle. (B) Sagittal T1 GE image of the central joint compartment: d, patella (note the cortical bone delineating the patella); e, patellar tendon; f, infrapatellar fat pad; g, cranial cruciate ligament; h, caudal cruciate ligament. (C) Sagittal T2-weighted SE image of the central joint compartment: g, cranial cruciate ligament; h, caudal cruciate ligament. (D) Dorsal T1-weighted SE image of the central joint compartment: g, cranial cruciate; h, caudal cruciate. (E) Sagittal T2-weighted spin echo (SE) image of the medial joint compartment: i, caudal horn of the medial meniscus; j, cranial horn of the medial meniscus; k, hyperintensity of a combination of joint fluid and articular cartilage. Note the hypointense line separating cartilage from trabecular bone corresponding to subchondral bone. (F) Sagittal T2-weighted SE image of the lateral joint compartment: i, caudal horn of the lateral meniscus; j, cranial horn of the lateral meniscus; l, extensor fossa. Note the hypointense line separating cartilage from trabecular bone corresponding to subchondral bone. (G) Sagittal T1 GE image of the medial joint compartment: i, caudal horn of the medial meniscus, note the hyperintensity of the central part; j, hyperintensity of the cranial horn of the medial meniscus; k, hyperintensity corresponding to joint fluid and articular cartilage. Note the hypointense line separating cartilage from trabecular bone corresponding to subchondral bone.

medial meniscus was smaller than the lateral meniscus in all dogs; however, measurements were not made. Menisci from 6 stifles with an inhomogeneous increase of intrameniscal signal were histologically normal.

## DISCUSSION

With the exception of poor delineation of articular cartilage, the protocol we used provided images of adequate quality to observe extra- and intraarticular structures in the normal canine stifle. MR images correlated well with observation of structures during gross dissection.

### *Dog Positioning*

Different dog positions were tried before we selected this protocol. Positioning is an important factor to improve observation intraarticular structures; some authors have positioned dogs in dorsal recumbency with the pelvic limb extended,<sup>14,17,18</sup> whereas others have used lateral recumbency.<sup>13</sup> In our experience, cruciate ligaments are best seen with the dogs positioned in lateral recumbency with 145° of stifle flexion, which places the cruciate ligaments under tension. Two previous MRI anatomic studies of the canine stifle used different low-field systems (0.064 T<sup>17</sup> and 0.5 T<sup>18</sup>). The main difference between these reports and our study is stifle position. In those studies, dogs were positioned in dorsal recumbency with pelvic extended or in 45° of flexion; however, the imaging protocol used was comparable. Nevertheless image quality differs among studies. Soler et al<sup>18</sup> published better quality images of ligamentous structures than Baird et al.<sup>17</sup> We tend to explain this by advances made in radiofrequency coil technology and in software between these reports published in 2007

hyperintense signal of joint fluid and distension of joint capsule increased contrast between ligaments and fluid allowing improving ligament identification (Fig 3C, C', C'' and D, D', D''). Image quality of the menisci was similar for both types of studies.

### *Comparison of MR Findings with Anatomic Dissection*

All MR images corresponded with gross dissection observation. All stifles were free of degenerative changes (osteophytes, cartilage erosion). The meniscofemoral ligament closely matched the MR images. Cruciate ligaments were normal and menisci were free of macroscopic lesions. The

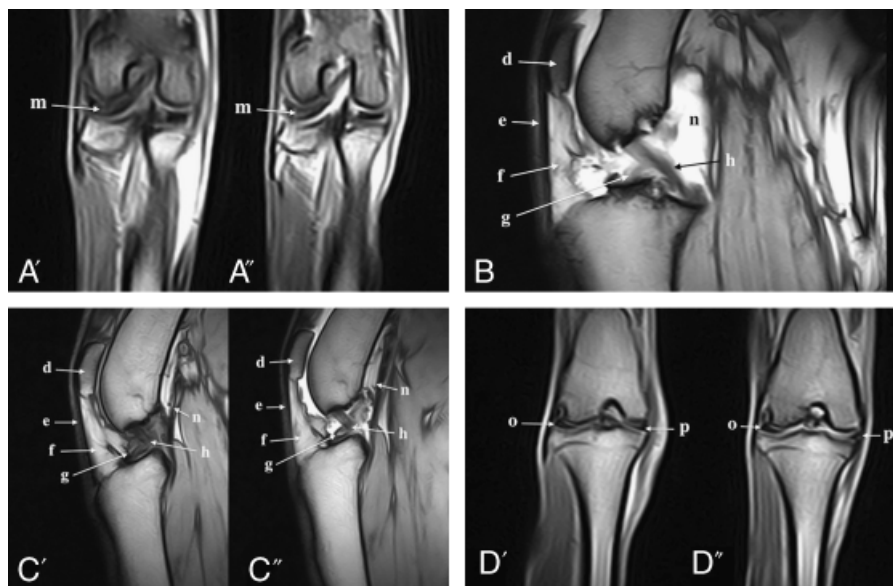


**Figure 3** (A) Dorsal T1-weighted spin echo (SE) image of conventional magnetic resonance imaging (MRI) (A') and MR arthrography (A'') of the caudal joint compartment: m, meniscofemoral ligament. (B) Sagittal T1 gradient echo (GE) MR arthrography of the central joint compartment: d, patella; e, patellar tendon; f, infrapatellar fat pad; g, cranial cruciate ligament; h, caudal cruciate ligament; n, distended joint capsule. (C) Sagittal T1 GE of conventional MRI (C') and MR arthrography (C'') of the central joint compartment: d, patella; e, patellar tendon; f, infrapatellar fat pad; g, cranial cruciate ligament; h, caudal cruciate ligament; n, joint capsule. (D) Dorsal T1-weighted SE of conventional MRI (D') and MR arthrography (D'') of the central joint compartment: o, lateral meniscus; p, medial meniscus.

and 1998, respectively. Our conventional MRI study is of comparable quality to Soler and colleagues.

### Image Quality

To improve image quality, an MR coil must adapt closely to the body region of interest.<sup>14</sup> This improves signal-to-noise ratio and, as a consequence, allows increased spatial resolution. Dedicated rigid extremity coils are used for MR of human knees providing the best quality image; however such coils designed for dogs were not available. The rigid extremity coil designed for human elbow that we used provided adequate images because it conformed closely to the dogs' stifle joint.

We found that images obtained in the dorsal and sagittal planes were most helpful to identify structures like cruciate ligaments and menisci, as reported by Blond et al.<sup>13</sup> The transverse plane was less helpful for assessing these structures. T1-weighted and T2-weighted SE sequences allowed excellent observation of anatomic detail of the joint and T1-weighted GE maximized signal and contrast between structures.

Our basic sequences using a standard software package were selected because they appeared to provide the quality required to properly image the normal canine stifle. It may be that imaging of pathologic joints with the same unit requires more sophisticated sequences. A recent study of diagnostic accuracy of high-field MRI for meniscal tears in dogs affected with naturally occurring cranial cruciate ligament rupture reported a global sensitivity of 100% and

specificity of 94% using proton density sequences,<sup>13</sup> the more sophisticated imaging protocol proposed in that study could be replicated for pathologic cases using a low-field unit. Nevertheless, the use of chemical fat saturation and special 3D GE sequences has become standard in human knee MR, and may become in dogs as well. Such sequences are currently not possible with low-field units.

The cranial cruciate ligament could not be seen in its entirety in the same image in all stifles, likely because of its oblique and spiral orientation within the joint. To limit this shortcoming, we did select an MR sagittal plane aligned with the cranial cruciate ligament. In contrast, the caudal cruciate ligament was seen in its entirety in all stifles probably because of its straight position.

In human MR imaging, the normal meniscus appears as low signal intensity on all sequences because of the low proton density of its fibrocartilage.<sup>4</sup> Canine menisci appear as wedge-shaped discs of fibrocartilage on sagittal and dorsal planes, with the lateral one larger than the medial one. All menisci were normal on gross dissection; however, 8 had a central increase of intrameniscal intensity without extension to the periphery in GE sequence. Menisci in these dogs were macroscopically normal and histology of 6 did not reveal any degenerative changes. Martig et al<sup>16</sup> reported that normal menisci had an inhomogeneous low signal intensity on GE sequences, a finding we agree with. It also corresponds to people where a higher internal signal can appear within the normal meniscus on GE sequences.<sup>3</sup> No rational explanation for this has been reported; one hypothesis about this central hyperintensity in GE could be

related to the composition of menisci and the vulnerability of GE sequences, producing this hyperintense effect. Another example of the vulnerability of GE sequences could be the thin hypointense band at the peripheral margins of the muscles and cartilage (or joint capsule) that may be linked to susceptibility artifacts. GE sequences should be interpreted with caution because of the high number of possible artifacts.

### MR Arthrography

We used diluted gadolinium similar to other veterinary studies<sup>14,25</sup> and because it is the contrast media used more frequently in people.<sup>1,8</sup> The imaging characteristics of intraarticular gadolinium confer certain advantages over saline solution, such as the capability of diagnosing a joint capsule tear on T1. Distension of joint capsule by this contrast media allowed hypointense structures (eg, cruciate ligaments, meniscomfemoral ligament, joint capsule), to stand out more easily against the hyperintense contrast media and joint fluid mixture. However, these were merely subjective observations on our part, with no scoring system.

Observation of menisci was not improved by MR arthrography likely because none of the dogs had macroscopic meniscal lesions. We simply aimed to explore the feasibility and advantages of MR arthrography in normal stifles. If a meniscal tear had been present, the contrast media would have likely filled the defects and a hyperintensity line crossing the meniscus would probably be seen, as reported.<sup>1,8</sup>

We chose to compare MR and MR arthrography images with gross dissection instead of arthroscopy because gross dissection provided advantages, such as removal of menisci and complete evaluation of all aspects, particularly the distal surface; and viewing of extracapsular structures like patella, patellar tendon, and collateral ligaments.

To our knowledge, a validated low-field MRI protocol to investigate articular cartilage does not exist in the veterinary literature. Boileau et al<sup>26</sup> reported a 3D spoiled gradient sequence with fat saturation with high-field magnet only used to perform quantitative measurement of cartilage volume in experimental canine stifle osteoarthritis. Canine stifle articular cartilage is very thin (0.6–1.3 mm) and it is difficult to differentiate with low-field units<sup>27</sup> and even with high-field units.<sup>28</sup> One might argue that the hyperintense line surrounding the hypointense subchondral bone in our dogs corresponded to articular cartilage as has been proposed<sup>17,18</sup>; however, observation of thin articular cartilage with a low-field unit is extremely difficult or impossible. We consider that the hyperintense zone identified in T2 and GE sequences in our dogs is a combination of joint fluid and articular cartilage.

### Limitations

Our study had limitations, one of which could be total imaging time. Seventy-five minutes may seem impractical

for clinical use; however, MR arthrography may not always be needed. Another limitation is the 4 mm slice thickness used. With low-field units, spatial resolution is limited with the same acquisition time, but acquisition time increases when slice thickness decreases. Our slice thickness can result in partial volume averaging and affect the conspicuity of small structures. However, we think that our slice thickness provides a good compromise between image quality and acquisition time. Moreover, image quality would decrease with thinner slices in small joints.

Our low-field MR protocol offers useful information on anatomic stifle structures in normal dogs and establishes the ability to investigate canine stifles with a low-field MR unit. We consider that the low-field MRI protocol we used provides images of adequate quality to assess the normal canine stifle joint. Nevertheless articular cartilage is not well delineated. Even though MR arthrography provides no additional information on normal menisci it may help diagnose meniscal injuries. This imaging protocol should be tested on pathologic joints and compared with high-field units to establish the diagnostic value of low-field MRI for stifles in dogs.

### ACKNOWLEDGMENTS

We thank Dr. Poujade for histologic examination of menisci.

### REFERENCES

1. Grainger AJ, Elliott JM, Campbell RS, et al: Direct MR arthrography: a review of current use. *Clin Radiol* 2000;55:163–176
2. Murphy WA, Totty WG: Musculoskeletal magnetic resonance imaging. *Magn Reson Annu* 1986, 1–35
3. Rubin DA, Paletta GA Jr.: Current concepts and controversies in meniscal imaging. *Magn Reson Imaging Clin N Am* 2000;8:243–270
4. Chan WP, Fritz RC, Stenibach SL, Wu CY, et al: The knee: internal derangements, in Saunders W, Chan WP, Lang P, Genant HK (eds) *MRI of the Musculoskeletal System*. Philadelphia, PA, Saunders, 1994, pp 263–306
5. Crues JV III., Mink J, Levy TL, Lotysch M, Stoller DW: Meniscal tears of the knee: accuracy of MR imaging. *Radiology* 1987;164:445–448
6. Mink JH, Levy T, Crues JV III.: Tears of the anterior cruciate ligament and menisci of the knee: MR imaging evaluation. *Radiology* 1988;167:769–774
7. Gylys-Morin VM, Hajek PC, Sartoris DJ, et al: Articular cartilage defects: detectability in cadaver knees with MR. *Am J Roentgenol* 1987;148:1153–1157
8. Steinbach LS, Palmer WE, Schweitzer ME: Special focus session. MR arthrography. *Radiographics* 2002;22:1223–1246
9. Helgason JW, Chandnani VP, Yu JS: MR arthrography: a review of current technique and applications. *Am J Roentgenol* 1997;168:1473–1480
10. Osinski T, Malfair D, Steinbach L: Magnetic resonance arthrography. *Orthop Clin N Am* 2006;37:299–319

11. Sahin G, Demirtas M: An overview of MR arthrography with emphasis on the current technique and applicational hints and tips. *Europ J Radiol* 2006;58:416–430
12. D'anjou MA, Moreau M, Troncy E, Martel-Pelletier J, et al: Osteophytosis, subchondral bone sclerosis, joint effusion and soft tissue thickening in canine experimental stifle osteoarthritis: comparison between 1.5 T magnetic resonance imaging and computed radiography. *Vet Surg* 2008;37:166–177
13. Blond L, Thrall DE, Roe SC, et al: Diagnostic accuracy of magnetic resonance imaging for meniscal tears in dogs affected with naturally occurring cranial cruciate ligament rupture. *Vet Radiol Ultrasound* 2008;49:425–431
14. Banfield CM, Morrison WB: Magnetic resonance arthrography of the canine stifle joint: technique and applications in eleven military dogs. *Vet Radiol Ultrasound* 2000;41:200–213
15. Baird DK, Hathcock JT, Kincaid SA, et al: Low-field magnetic resonance imaging of early subchondral cyst-like lesions in induced cranial cruciate ligament deficient dogs. *Vet Radiol Ultrasound* 1998;39:167–173
16. Martig S, Konar M, Schmökel HG, et al: Low-field MRI and arthroscopy of meniscal lesions in ten dogs with experimentally induced cranial cruciate ligament insufficiency. *Vet Radiol Ultrasound* 2006;47:515–522
17. Baird DK, Hathcock JT, Rumph PF, et al: Low-field magnetic resonance imaging of the canine stifle joint: normal anatomy. *Vet Radiol Ultrasound* 1998;39:87–97
18. Soler M, Murciano J, Latorre R, et al: Ultrasonographic, computed tomographic and magnetic resonance imaging anatomy of the normal canine stifle joint. *Vet J* 2007; 174:351–361
19. Nordberg CC, Johnson KE: Magnetic resonance imaging of normal canine carpal ligaments. *Vet Radiol Ultrasound* 1999;40:128–136
20. Snaps FR, Saunders JH, Park RD, et al: Comparison of spin echo, gradient echo and fat saturation magnetic resonance imaging sequences for imaging the canine elbow. *Vet Radiol Ultrasound* 1998;39:518–523
21. Schaefer SL, Forrest LJ: Magnetic resonance imaging of the canine shoulder: an anatomic study. *Vet Surg* 2006;35: 721–728
22. Tivers MS, Mahoney P, Corr SA: Canine stifle positive contrast computed tomography arthrography for assessment of caudal horn meniscal injury: a cadaver study. *Vet Surg* 2008;37:269–277
23. Samii V, Dyce J, Pozzi A, et al: Computed tomographic arthrography of the stifle for detection of cranial and caudal cruciate ligament and meniscal tears in dogs. *Vet Radiol Ultrasound* 2009;50:144–150
24. Tivers MS, Mahoney P, Baines S, et al: Diagnostic accuracy of positive contrast computed tomography arthrography for the detection of injuries to the medial meniscus in dogs with naturally occurring cranial cruciate ligament insufficiency. *J Small Anim Pract* 2009;50:324–332
25. Murphy SE, Ballegeer EA, Forrest LJ, et al: Magnetic resonance imaging findings in dogs with confirmed shoulder pathology. *Vet Surg* 2008;37:631–638
26. Boileau C, Martel-Pelletier J, Abram F, et al: Magnetic resonance imaging can accurately assess the long-term progression of knee structural changes in experimental dog osteoarthritis. *Ann Rheum Dis* 2008;67:926–932
27. Frisbie DD, Cross MW, McIlwraith CW: A comparative study of articular cartilage thickness in the stifle of animal species used in human pre-clinical studies compared to articular cartilage thickness in the human knee. *Vet Comp Orthop Traumatol* 2006;19:142–146
28. Janach KJ, Breit SM, Künzel WW: Assessment of the geometry of the cubital (elbow) joint of dogs by use of magnetic resonance imaging. *Am J Vet Res* 2006;67:211–218